AIMS Mathematics, 8(8): 18846–18865.
DOI:10.3934/math.2023959
Received: 14 March 2023
Revised: 25 April 2023
Accepted: 27 April 2023
Published: 05 June 2023

http://www.aimspress.com/journal/Math

Research article

Mathematical analysis of neurological disorder under fractional order derivative

Nadeem Khan[1], Amjad Ali[1], Aman Ullah[2] and Zareen A. Khan[3,*]

[1] Department of Basic Sciences & Islamiat, University of Engineering and Technology, Peshawar, Pakistan
[2] Department of Mathematics, University of Malakand, Dir(L), Khyber Pakhtunkhwa, Pakistan
[3] Department of Mathematical Sciences, College of Science, Princess Nourah bint Abdulrahman University, P. O. Box 84428, Riyadh 11671, Saudi Arabia

* **Correspondence:** Email: zakhan@pnu.edu.sa.

Abstract: Multiple sclerosis (MS) is a common neurological disorder that affects the central nervous system (CNS) and can cause lesions that spread over space and time. Our study proposes a mathematical model that illustrates the progression of the disease and its likelihood of recurrence. We use Caputo fractional-order (FO) derivative operators to represent non-negative solutions and to establish a steady-state point and basic reproductive number. We also employ functional analysis to prove the existence of unique solutions and use the Ulam-Hyres (UH) notion to demonstrate the stability of the solution for the proposed model. Furthermore, we conduct numerical simulations using an Euler-type numerical technique to validate our theoretical results. Our findings are presented through graphs that depict various behaviors of the model for different parameter values.

Keywords: fractional operator; existence theory; numerical method; unique solution
Mathematics Subject Classification: 26A33, 34K37

1. Introduction and motivation

Multiple sclerosis (MS) is an autoimmune neurological disorder that affects the central nervous system (CNS) and primarily damages oligodendryocytes, which are myelin producing cells. This damage leads to dysfunction of neurons in the brain and spinal cord, causing various neurological symptoms. It is commonly accepted that MS is an unpredictable illness that can have permanent effects on the brain, spinal cord, and optic nerves. Symptoms may include difficulty with movement, cloudy vision, and further neurological issues. The severity and deductability of signs can vary greatly from patient to patient, ranging from subtle cases that require no medical intervention to severe cases that

disrupt daily activities and require relapse-preventive therapies. Shigesi et al. [1] studied the association between endometriosis and autoimmune disease. Similar studies can be found in [2–4].

MS is classified as an autoimmune neurodegenerative condition, which is characterized by the degeneration of axons and neurons, demyelination, and inflammation in the CNS. The direct cause of MS is largely unknown; although there are treatments available to slow the progression of MS and limit any further damage to the CNS, there is currently no overall cure. The disease has been attributed to a variety of factors, including immune dysfunction, viral infection, and genetic, epigenetic, and environmental factors. Typically, symptoms of MS first present in patients between the ages of 15 and 50.

Relapsing-remitting MS (RRMS) is the most prevalent form of MS, characterized by episodes of neurological symptoms, followed by periods of remission. MS is approximately three times more common in females than males, and predicting the clinical course of relapses remains a challenge due to the variability of the disease and the influence of factors such as a sick person's environment, lab findings, and medical profile. Kaiko et al. [5] analyzed immunological decision making, and the relation between dendritic cells and cytokines was investigated by the authors in [6]. More analysis on this aspect can be found in [7, 8].

The neurological damaged caused by MS can be classified in two ways: slow progressive brain degeneration and regular attacks (relapses). Usually classified as a combination of at least two of these parts, the clinical direction in MS patients are mostly categorized into three different forms: the primary progressive phase (PPMS), the RRMS phase, and the secondary progressive phase (SPMS) [9].

PPMS and RRMS have contrasting symptoms. PPMS is characterized by a gradual decline in cerebral function starting from the early stages of the disease, without clear-cut episodes of clinical relapse [10, 11]. In contrast, RRMS is characterized by clinical relapses that occur unpredictably, leading to temporary episodes of cerebral weakening [12, 13].

Because the adoptive immune system reacts against non-self, the immune system must be able to recognize self from non-self; otherwise, an extensive range of immune diseases can occur. Through the development of the immune system, different levels of immune reactions against non-self can lead to variations of mechanisms form one end of the spectrum to another [14]. Various disease-modifying drugs (DMDs), such as fingolimod, natalizumab, and interferon, have demonstrated an impressive efficacy in reducing relapse rates in patients with multiple sclerosis.

However, not all individuals with MS will benefit from these DMDs. Additionally, DMDs are helpful for proscribe relapse, since certain patients with MS have not been able to effectively block the progressive brain decay connected with relapse. Additional research toward understanding the pathophysiological mechanisms of MS can be beneficial in producing additional treatments.

Therefore, developing an accurate mathematical model that mimics the clinical manifestations of MS is a promising approach.

Some mathematical models have been constructed to elucidate the perplexing concentric morphology of demyelinating lesions. The focus of these models is on how macrophages are activated and recruited in relation to the development of demyelinating lesions [15, 16]. Another model has been introduced to illustrate the manifestation of cerebral decline lesions in demyelinating diseases, and incorporating the dynamic interactions among macrophages, chemoattractants, and destroyed oligodendrocyte in the brain volume. However, to analyze the non-linear asymmetrical laboratory case and the dispersed distribution of lesions in MS, the authors in [17] constructed a new system that

considers the specific uncertainties in space and time. We recall the following model proposed in [17] described below.

Let $\mathbb{P}(t)$ represent the ratio of normal (healthy) brain cells (NBC), $\mathbb{I}(t)$ represent the infected brain cells (IBC), and $\mathbb{Q}(t)$ represent the damaging (either immune or viral effectors) brain cells (DBC).

In addition, let γ denote the growth rate of NBC. Based on scientific observations, either viruses or immune cells contribute to the development of this disease. Therefore, we assume that infected cells $\mathbb{I}(t)$ release the virus $\mathbb{Q}(t)$ at a rate of δ and expire at a rate of α. The virus $\mathbb{Q}(t)$ is influenced by NBC $\mathbb{P}(t)$ at a rate of d and expires at a rate of κ. We assume that d is small and the control parameters β, γ, δ belong to that domain where $\mathbb{P}$, $\mathbb{I}$, $\mathbb{Q}$, are non-negative. Therefore, the mathematical system can be expressed in the following form [17]:

$$\begin{cases} \frac{d}{dt}\mathbb{P} &= \gamma\mathbb{P}(1-\mathbb{P}) - \beta\mathbb{P}\mathbb{Q}, \\ \frac{d}{dt}\mathbb{I} &= \beta\mathbb{P}\mathbb{Q} - \alpha\mathbb{I}, \\ \frac{d}{dt}\mathbb{Q} &= \delta\mathbb{I} - d\mathbb{P}\mathbb{Q} - \kappa\mathbb{Q}. \end{cases} \tag{1.1}$$

In the field of epidemiology, there has been a recent trend of using fractional-order (FO) derivatives and integral operators in mathematical models. These operators are more flexible than traditional deterministic models and have been a focus of current research in mathematics. Shah et al. investigated Pine Wilt disease and COVID-19 models under FO [18, 19]. Beside this, FO operators have been used in the analysis and applications of delay differential equations. For instance, Xu et al. demonstrated a FO 4D neural network including two different delays [20] and three-triangle multi-delayed neural networks [21]. Additionally, we suggest two works on FO delay differential equations [22, 23].

FO differential equations involve either fractional-order derivatives or integral operators that depend on past states as well as current states, making them a powerful tool for predicting future states. They are more effective than classical deterministic operators, and Caputo and Riemann-Liouville operators are commonly used in fractional-order differential equations. There are several applications of differential equations in science and technology. For instance, several authors have used FO to analyze wave behaviours in mathematical physics problems such as Schrodinger's equation [24], biophysics [25], nonlinear evolution equations [26], fractional wave equations [27], time-fractional Fornberg-Whitham and Klein-Gordon equations [28], and fluid dynamics [29]. FO can be applied to bifurcations and chaos analyses of dynamical systems. The advantage of FO over the integer order operator in chaos analysis is that it provides more advanced features in chaotic dynamical systems that are not attainable at integer order. Here, we give some applications of FO in bifurcation and chaos analysis, such as: 4D-hyperchaotic system [30], coupled memristive model [31], 4D-memristive system [32] and chaos in predator prey model [33].

In epidemiology, integer operators are basic tools for modelling the dynamics of a disease [34]. However, FO has been used by many researchers for an improved prediction and analysis of numerous disease models, such as a tumor-immune model [35], bacteria dependent disease [36], a COVID-19 model [37], Buruli ulcers [38], a COVID-19 model for a case study in Saudi Arabia [39], HBV and HCV co-infection models [40], a Vector-host disease model [41], a compartmental disease model [42], and many more [43, 44].

In the next section, we propose a simple mathematical model consisting of three simultaneous fractional differential equations that can replicate the clinical presentation of MS. In developing our model, we draw upon previous research on Ulam-Hyers stability and the instability of steady state

solutions and pattern formation. We derive conditions for the existence, uniqueness, and stability of steady states both at equilibrium and away from equilibrium. We then use numerical simulation techniques to verify our theoretical results. Finally, in the concluding section, we summarize our findings and conclude our study.

The structure of the paper is as follows: In Section 2, we introduce the fundamental concepts of fractional calculus. In Section 3, we present the primary findings of our research, comprised of a theoretical and numerical analysis of the proposed model. In Section 4, we present the numerical simulations. Finally, in Section 5, we provide the concluding remarks.

2. Preliminaries

Here, we provide a definition of some fractional operators.

Definition 2.1. *[45] Let* $\Psi(t) \in C[0,T]$, *then the Caputo operator is defined as:*

$$ {}^{C}\mathcal{D}_t^{\mu}\Psi(t) = \frac{1}{\Gamma(1-\mu)}\int_0^t (t-a)^{-\mu}\frac{d}{da}\Psi(a)da. \tag{2.1}$$

Definition 2.2. *[45] Let* $\Psi \in L^1([0,\boldsymbol{T}],\mathbb{R})$, *the Reimann-Liouville fractional integral operator of* $0<\mu\leq 1$ *order is defined as:*

$$\mathcal{I}_t^{\mu}\Psi(t) = \frac{1}{\Gamma(\mu)}\int_0^t (t-a)^{\mu-1}\Psi(a)\,da.$$

Definition 2.3. *[45] The Reimann-Liouville fractional derivative of order* μ *is expressed by:*

$$\mathcal{D}_t^{\mu}\Psi(t) = \frac{1}{\Gamma(1-\mu)}\frac{d}{dt}\int_0^t \frac{\Psi(a)}{(t-a)^{\mu}}da.$$

3. Main work

Here, the classical derivative in the model (1.1) is replaced by the Caputo fractional-order RRMS model, described as:

$$\begin{cases} {}^{C}\mathcal{D}_t^{\mu}\mathbb{P}(t) &= \gamma\mathbb{P}(1-\mathbb{P}) - \beta\mathbb{P}\mathbb{Q}, \\ {}^{C}\mathcal{D}_t^{\mu}\mathbb{I}(t) &= \beta\mathbb{P}\mathbb{Q} - \alpha\mathbb{I}, \\ {}^{C}\mathcal{D}_t^{\mu}\mathbb{Q}(t) &= \delta\mathbb{I} - d\mathbb{P}\mathbb{Q} - \kappa\mathbb{Q}, \end{cases} \tag{3.1}$$

along with initial conditions:

$$\mathbb{P}(0) = \mathbb{P}_0, \mathbb{I}(0) = \mathbb{I}_0, \mathbb{Q}(0) = \mathbb{Q}_0.$$

Since model (3.1) is nonlinear and lacks a time-dependent explicit solution, it is studied over a prolonged time period. By setting the derivatives of model (3.1) equal to zero, we obtain the following equilibria:

$\mathbb{E}_0 = (0,0,0)$, $\mathbb{E}_1 = (1,0,0)$, and $\mathbb{E}_2 = \left(\frac{\alpha\kappa}{(\beta\delta-\alpha d)}, \frac{\gamma\kappa(\beta\delta-\alpha d-\alpha\kappa)}{(\beta\delta-\alpha d)^2}, \frac{\gamma(\beta\delta-\alpha d-\alpha\kappa)}{\beta(\beta\delta-\alpha d)}\right)$, also, the basic reproduction number is given as:

$$\mathbb{R}_0 = \frac{\delta\beta}{\alpha(d+\kappa)}.$$

3.1. Non-negativity of solutions

This portion focuses on the existence of a non-negative solution for the fractional order RRMS model. It is evident from biological considerations that each state variable in the model (3.1) represents a non-negative real-valued function. Stated differently, $(\mathbb{P}(t), \mathbb{I}(t), \mathbb{Q}(t)) \in \mathbb{R}^3_+$ where

$$\mathbb{R}^3_+ = \left\{x = (x_1, x_2, x_3) : x_j \geq 0, \forall i = 1, 2, 3\right\}.$$

First, we will demonstrate that all solutions of the model (3.1) are non-negative.

Theorem 3.1. *All solutions of the considered FO RRMS model (3.1) belong to the non-negative real space* $\mathbb{R}^3_+$.

Proof. Consider the RRMS model (3.1), we have

$$\begin{cases} {}^C\mathcal{D}^{\mu}_t \mathbb{P}(t)_{|_{\mathbb{P}(t)=0}} = 0, \text{ where } 0 < \gamma \leq 1 \text{ and } \mathbb{X} \geq 0, \\ {}^C\mathcal{D}^{\mu}_t \mathbb{I}(t)_{|_{I(t)=0}} = \beta\mathbb{P}\mathbb{Q} \geq 0, \text{ where } \mathbb{P}(t) \geq 0 \text{ and } \beta > 0 \\ {}^C\mathcal{D}^{\mu}_t \mathbb{Q}(t)_{|_{\mathbb{Q}(t)=0}} = \delta\mathbb{I} \geq 0, \text{ where } \delta > 0 \text{ and } \mathbb{I} \geq 0. \end{cases}$$

Using fractional integral, we will get the solution of the above systems. The solution will be nonnegative since there is no negative term in the system. □

3.2. Existence and uniqueness theorems

In this part, we will find the existence of a solution for the considered FO RRMS model (3.1) via the concepts of the fixed- point theory. Define a norm as:

$$\| (\mathbb{P}, \mathbb{I}, \mathbb{Q}) \| = \| \mathbb{P} \| + \| \mathbb{I} \| + \| \mathbb{Q} \|,$$

where $\| \mathbb{P} \| = sup \{| \mathbb{P}(t) |: t \in \mathrm{T}\}$, $\| \mathbb{I} \| = sup \{| \mathbb{I}(t) |: t \in \mathrm{T}\}$, $\| \mathbb{Q} \| = sup \{| \mathbb{Q}(t) |: t \in \mathrm{T}\}$, and $A = (c[0, \mathrm{T}])$, where $(c[0, \mathrm{T}])$ denotes the Banach space of real value continues mapping on T in the related supremum norm. Let us express the model (3.1) as:

$$\begin{cases} {}^C\mathcal{D}^{\mu}_t \mathbb{P}(t) &= \mathcal{Q}_1(t, \mathbb{P}), \\ {}^C\mathcal{D}^{\mu}_t \mathbb{I}(t) &= \mathcal{Q}_2(t, \mathbb{I}), \\ {}^C\mathcal{D}^{\mu}_t \mathbb{Q}(t) &= \mathcal{Q}_3(t, \mathbb{Q}). \end{cases} \tag{3.2}$$

By applying the definition of fractional integral of model (3.2) and using the properties of fractional calculus we get

$$\begin{cases} \mathbb{P}(t) - \mathbb{P}(0) &= \frac{1}{\Gamma(1-\mu)} \int_0^t (t-a)^{-\mu} \mathcal{Q}_1(t, \mathbb{P}) da \\ \mathbb{I}(t) - \mathbb{I}(0) &= \frac{1}{\Gamma(1-\mu)} \int_0^t (t-a)^{-\mu} \mathcal{Q}_2(t, \mathbb{I}) da \\ \mathbb{Q}(t) - \mathbb{Q}(0) &= \frac{1}{\Gamma(1-\mu)} \int_0^t (t-a)^{-\mu} \mathcal{Q}_3(t, \mathbb{Q}) da, \end{cases} \tag{3.3}$$

where $t \in [0, \mathrm{T}]$ and $0 < \mu \leq 1$ with the following theorem, we will assume that $\| \mathbb{P}(t) \| \leq c_1$, $\| \mathbb{I}(t) \| \leq c_2$, and $\| \mathbb{Q}(t) \| \leq c_3$ where c_i, $i = 1, 2, 3$ are positive constants

$$\mathrm{m}_1 = \gamma - \beta c_3 - 2\gamma c_1, \mathrm{m}_2 = \alpha, \mathrm{m}_3 = dc_1 + k.$$

Theorem 3.2. *Assume that* $0 \leq max\{m_1, m_2, m_3\} < 1$, *then we show that kernels* $\mathscr{Q}_1$, $\mathscr{Q}_2$, $\mathscr{Q}_3$ *agrees to fulfill the Lipschitz constraint and are contractions under some mappings.*

Proof. Consider $\mathbb{P}_1$ and $\mathbb{P}_2$ be any functions, then we have

$$\begin{aligned}
\|\mathscr{Q}_1(t,\mathbb{P}_1) - \mathscr{Q}_1(t,\mathbb{P}_2)\| &\leq \|\gamma\mathbb{P}_1(t)(1-\mathbb{P}_1(t)) - \beta\mathbb{P}_1(t)\mathbb{Q}(t) - \gamma\mathbb{P}_2(t)(1-\mathbb{P}_2(t)) + \beta\mathbb{P}_2(t)\mathbb{Q}(t)\| \\
&= \left\|\gamma\mathbb{P}_1(t) - \gamma\mathbb{P}_1^2(t) - \beta\mathbb{P}_1(t)\mathbb{Q}(t) - \gamma\mathbb{P}_2(t) + \gamma\mathbb{P}_2^2(t) + \beta\mathbb{P}_2(t)\mathbb{Q}(t)\right\| \\
&= \left\|\gamma(\mathbb{P}_1(t) - \mathbb{P}_2(t)) - \beta\mathbb{Q}(t)(\mathbb{P}_1(t) - \mathbb{P}_2(t)) - \gamma\left(\mathbb{P}_1^2(t) - \mathbb{P}_2^2(t)\right)\right\| \\
&= \|(\gamma - \beta\mathbb{Q}(t))(\mathbb{P}_1(t) - \mathbb{P}_2(t)) - \gamma(\mathbb{P}_1(t) + \mathbb{P}_2(t))(\mathbb{P}_1(t) - \mathbb{P}_2(t))\| \\
&= \|\gamma - \beta\mathbb{Q}(t) - \gamma(\mathbb{P}_1(t) + \mathbb{P}_2(t))(\mathbb{P}_1(t) - \mathbb{P}_2(t))\| \\
&\leq \|\gamma - \beta\mathbb{Q}(t) - \gamma(\mathbb{P}_1(t) + \mathbb{P}_2(t))\|\,\|(\mathbb{P}_1(t) - \mathbb{P}_2(t))\| \\
&\leq \gamma - \beta\|\mathbb{Q}(t)\| - \gamma(\|\mathbb{P}_1(t)\| + \|\mathbb{P}_2(t)\|)\|\mathbb{P}_1 - \mathbb{P}_2\| \\
&\leq \gamma - \beta C_3 - \gamma(2C_1)\|\mathbb{P}_1 - \mathbb{P}_2\| \\
&\leq \mathrm{m}_1\|\mathbb{P}_1 - \mathbb{P}_2\|,
\end{aligned}$$

which implies that

$$\|\mathscr{Q}_1(t,\mathbb{P}_1) - \mathscr{Q}_1(t,\mathbb{P}_2)\| \leq \mathrm{m}_1\|\mathbb{P}_1 - \mathbb{P}_2\|. \tag{3.4}$$

Therefore, the Lipschitz condition is fulfilled. Similarly, the kernels $\mathscr{Q}_2, \mathscr{Q}_3$, can be fined using $\{\mathbb{I}_1, \mathbb{I}_2\}$ and $\{\mathbb{Q}_1, \mathbb{Q}_2\}$.

$$\begin{cases}
\|\mathscr{Q}_1(t,\mathbb{P}_1) - \mathscr{Q}_1(t,\mathbb{P}_2)\| & \leq \mathrm{m}_1\|\mathbb{P}_1 - \mathbb{P}_2\| \\
\|\mathscr{Q}_2(t,\mathbb{I}_1) - \mathscr{Q}_2(t,\mathbb{I}_2)\| & \leq \mathrm{m}_2\|\mathbb{I}_1 - \mathbb{I}_2\| \\
\|\mathscr{Q}_3(t,\mathbb{Q}_1) - \mathscr{Q}_3(t,\mathbb{Q}_2)\| & \leq \mathrm{m}_3\|\mathbb{Q}_1 - \mathbb{Q}_2\|.
\end{cases}$$

In addition, since $0 \leq max\{\mathrm{m}_1, \mathrm{m}_2, \mathrm{m}_3\} < 1$, the kernel are contractions. Recursively, system (3.3) can be given as

$$\begin{cases}
\mathbb{X}_{\mathrm{n}}(t) - \mathbb{P}(0) &= \frac{1}{\Gamma(1-\mu)}\int_0^t (t-a)^{-\mu}\,\mathscr{Q}_1(a,\mathbb{P}_{n-1})\,da, \\
\mathbb{I}_{\mathrm{n}}(t) - \mathbb{I}(0) &= \frac{1}{\Gamma(1-\mu)}\int_0^t (t-a)^{-\mu}\,\mathscr{Q}_2(a,\mathbb{I}_{n-1})\,da, \\
\mathbb{Z}_{\mathrm{n}}(t) - \mathbb{Q}(0) &= \frac{1}{\Gamma(1-\mu)}\int_0^t (t-a)^{-\mu}\,\mathscr{Q}_3(a,\mathbb{Q}_{n-1})\,da.
\end{cases} \tag{3.5}$$

Let

$$\mathcal{K}(t) = \begin{pmatrix} \mathbb{P}(t) \\ \mathbb{I}(t) \\ \mathbb{Q}(t) \end{pmatrix},$$

$$Z(t,\mathcal{K}(t)) = \begin{pmatrix} \mathscr{Q}_1(t,\mathbb{P}_1) \\ \mathscr{Q}_2(t,\mathbb{I}_1) \\ \mathscr{Q}_3(t,\mathbb{Q}_1) \end{pmatrix},$$

$$\mathcal{K}(0) = \begin{pmatrix} \mathbb{P}(0) \\ \mathbb{I}(0) \\ \mathbb{Q}(0) \end{pmatrix}.$$

Using (3.5), we obtain the following formation:

$$\mathcal{K}(t) = \mathcal{K}_0 + \frac{1}{\Gamma(\mu)}\int_0^t (t-a)^{\mu-1} Z(a,\mathcal{K}(a))da. \tag{3.6}$$

The difference between the successive terms of model (3.2) in the recursive form is defined as:

$$\begin{aligned}
\Phi_{1n}(t) &= \mathbb{X}_{\mathrm{n}}(t) - \mathbb{X}_{\mathrm{n-1}}(t) \\
&= \frac{1}{\Gamma(1-\mu)} \int_0^t (t-a)^{-\mu} \mathcal{Q}_1(a,\mathbb{P}_{n-1}) - \mathcal{Q}_1(a,\mathbb{P}_{n-2})\, da \\
\Phi_{2n}(t) &= \mathbb{I}_{\mathrm{n}}(t) - \mathbb{I}_{\mathrm{n-1}}(t) \\
&= \frac{1}{\Gamma(1-\mu)} \int_0^t (t-a)^{-\mu} \mathcal{Q}_2(a,\mathbb{I}_{n-1}) - \mathcal{Q}_2(a,\mathbb{I}_{n-2})\, da \\
\Phi_{3n}(t) &= \mathbb{Z}_{\mathrm{n}}(t) - \mathbb{Z}_{\mathrm{n-1}}(t) \\
&= \frac{1}{\Gamma(1-\mu)} \int_0^t (t-a)^{-\mu} \mathcal{Q}_3(a,\mathbb{Q}_{n-1}) - \mathcal{Q}_3(a,\mathbb{Q}_{n-2})\, da,
\end{aligned}$$

with the initial condition $\mathbb{P}_0(t) = \mathbb{P}(0)$, $\mathbb{I}_0(t) = \mathbb{I}(0)$, $\mathbb{Q}_0(t) = \mathbb{Q}(0)$. By using the norm of the equation, we have

$$\begin{aligned}
\|\Phi_{1n}(t)\| &= \|\mathbb{X}_{\mathrm{n}}(t) - \mathbb{X}_{\mathrm{n-1}}(t)\| \\
&= \left\| \frac{1}{\Gamma(1-\mu)} \int_0^t (t-a)^{-\mu} \mathcal{Q}_1(a,\mathbb{P}_{n-1}) - \mathcal{Q}_1(a,\mathbb{P}_{n-2})\, da \right\| \\
&\leq \frac{1}{\Gamma(1-\mu)} \left\| \int_0^t (t-a)^{-\mu} \mathcal{Q}_1(a,\mathbb{P}_{n-1}) - \mathcal{Q}_1(a,\mathbb{P}_{n-2})\, da \right\|.
\end{aligned}$$

According to the Lipschitz condition (3.4), we get

$$\|\mathbb{X}_{\mathrm{n}}(t) - \mathbb{X}_{\mathrm{n-1}}(t)\| \leq \frac{1}{\Gamma(1-\mu)} \mathrm{m}_1 \int_0^t (t-a)^{-\mu} \|\mathbb{X}_{\mathrm{n-1}}(t) - \mathbb{X}_{\mathrm{n-2}}(t)\|\, da.$$

Thus, we have

$$\|\Phi_{1n}(t)\| \leq \frac{1}{\Gamma(1-\mu)} \mathrm{m}_1 \int_0^t (t-a)^{-\mu} \left\|\Phi_{1(n-1)}(a)\right\| da. \tag{3.7}$$

Similarly, the Lipschitz property for the remaining equation of the model can be obtained with

$$\begin{cases}
\|\Phi_{2n}(t)\| & \leq \frac{1}{\Gamma(1-\mu)} \mathrm{m}_2 \int_0^t (t-a)^{-\mu} \left\|\Phi_{2(n-1)}(a)\right\| da, \\
\|\Phi_{3n}(t)\| & \leq \frac{1}{\Gamma(1-\mu)} \mathrm{m}_3 \int_0^t (t-a)^{-\mu} \left\|\Phi_{3(n-1)}(a)\right\| da.
\end{cases} \tag{3.8}$$

The properties of the kernel, as shown in Eq (3.4), have been established and holds. By analysing the remainder of Eqs (3.7) and (3.8), and applying the recursive access, we get the output as:

$$\begin{cases}
\|\Phi_{1n}(t)\| & \leq \|\mathbb{P}_0(t)\| \left[\frac{1}{\Gamma(1-\mu)} \mathrm{m}_1 p^{1-\mu}\right]^n \\
\|\Phi_{2n}(t)\| & \leq \|\mathbb{I}_0(t)\| \left[\frac{1}{\Gamma(1-\mu)} \mathrm{m}_2 p^{1-\mu}\right]^n \\
\|\Phi_{3n}(t)\| & \leq \|\mathbb{Q}_0(t)\| \left[\frac{1}{\Gamma(1-\mu)} \mathrm{m}_1 p^{1-\mu}\right]^n.
\end{cases} \tag{3.9}$$

Therefore, the existing and given sequence follows $\|\Phi_{1n}(t)\| \to 0$, $\|\Phi_{2n}(t)\| \to 0$ and $\|\Phi_{3n}(t)\| \to 0$ as $n \to \infty$. Therefore, at least one solution exists for the considered model.

$$\begin{cases}
\mathbb{P}_n(t) & = \sum_{i=1}^n \Phi_{1n}(t) \\
\mathbb{I}_n(t) & = \sum_{i=1}^n \Phi_{2n}(t) \\
\mathbb{Q}_n(t) & = \sum_{i=1}^n \Phi_{3n}(t).
\end{cases}$$

□

We propose the following results, which guarantees the unique solution of model (3.2).

Theorem 3.3. *The Caputo-fractional* (*RRMS*) *model (3.2) has a unique solution for* $t \in [0, \mathrm{T}]$ *if the inequality exists* $\frac{1}{\Gamma(1-\mu)} p^{1-\mu} \mathrm{m}_1 < 1$, *where* $i = 1, 2, 3$.

Proof. To prove the uniqueness of the solution, considering Eq (3.9) and taking triangular inequality for any $i = 1, 2, 3$, we have

$$\begin{cases} \|\mathbb{X}_{\mathrm{n+i}}(\mathrm{t}) - \mathbb{X}_{\mathrm{n}}(t)\| & \leq \sum_{k=n+1}^{n+i} \mathrm{m}_1^i = \frac{\mathrm{m}_1^{n+1} - \mathrm{m}_1^{n+i+1}}{1-\mathrm{m}_1} \\ \|\mathbb{I}_{\mathrm{n+i}}(\mathrm{t}) - \mathbb{I}_{\mathrm{n}}(t)\| & \leq \sum_{k=n+1}^{n+i} \mathrm{m}_2^i = \frac{\mathrm{m}_2^{n+1} - \mathrm{m}_2^{n+i+1}}{1-\mathrm{m}_2} \\ \|\mathbb{Z}_{\mathrm{n+i}}(\mathrm{t}) - \mathbb{Z}_{\mathrm{n}}(t)\| & \leq \sum_{k=n+1}^{n+i} \mathrm{m}_3^i = \frac{\mathrm{m}_3^{n+1} - \mathrm{m}_3^{n+i+1}}{1-\mathrm{m}_3}, \end{cases} \tag{3.10}$$

where $\frac{1}{\Gamma(1-\mu)} \mathrm{m}_1 p^{1-\mu} < 1$ by assertion and $\mathrm{m}_i = \left[\frac{1}{\Gamma(1-\mu)} \mathrm{m}_1 p^{1-\mu}\right]^n$, $i = 1, 2, 3$. Therefore, the sequences $\mathbb{P}_n$, $\mathbb{I}_n$, $\mathbb{Q}_n$ behave as Cauchy sequences in $\mathbb{M}(k)$, and as such, they converge uniformly. By applying the limit theory to Eq (3.10) as $n \to \infty$, the limit of these sequences gives a unique solution to model (3.1). Thus, the existence of a unique solution for model (3.1) has been proven. □

3.3. Ulam-Hyers stability

This section will cover the various forms of UH stability (UHS) and gives definitions for some UHS criteria for the proposed system. Let $\mathcal{K} \in A$ be any solution of the considered FO RRMS model (3.1), and $\varepsilon > 0$ and $\mathcal{L}_Z : [0, \boldsymbol{T}] \times \mathbb{R}^3 \to \mathbb{R}^+$ shows a continuous function. We are presented with a set of inequalities:

$$\left|{}^C\mathcal{D}_t^\mu \mathbb{M}(t) - \mathbb{Q}(t, \mathbb{M}(t))\right| \leq \varepsilon, \tag{3.11}$$

$$\left|{}^C\mathcal{D}_t^\mu \mathbb{M}(t) - \mathbb{Q}(t, \mathbb{M}(t))\right| \leq \varepsilon \mathcal{L}_Z(t), \tag{3.12}$$

$$\left|{}^C\mathcal{D}_t^\mu \mathbb{M}(t) - \mathbb{Q}(t, \mathbb{M}(t))\right| \leq \mathcal{L}_Z(t), \tag{3.13}$$

where $t \in [0, \boldsymbol{T}]$ and $\varepsilon = \max(\varepsilon_i)^{\boldsymbol{T}}$ for $i = 1, 2, 3$.

Definition 3.4. *The given FO RRMS model (3.1) will be UHS if* $\forall\ \varepsilon > 0$, *and* $\forall$ *solution* $\mathbb{M} \in A$ *of system (3.3)* $\exists\, \mathcal{J}_Z > 0$ *such that*

$$|\mathbb{M}(t) - \mathcal{K}(t)| \leq \varepsilon \mathcal{J}_Z > 0,$$

where $\mathcal{J}_Z = \max(\mathcal{J}_{Z_i})^{\boldsymbol{T}}$.

Definition 3.5. *The proposed RRMS model (3.1) will be a generalized UHS if* $\exists$ *a function* $\mathcal{H}_Z$ *with* $\mathcal{H}_{\mathcal{Z}}(0) = 0$ *such that*

$$|\mathbb{M}(t) - \mathcal{K}(t)| \leq \mathcal{H}_Z(\varepsilon),$$

where $\mathcal{H}_Z = \max(\mathcal{H}_{Z_i})^{\boldsymbol{T}}$ *for* $i = 1, 2, 3$.

Definition 3.6. *The given RRMS model (3.1) will be a UHRS if* $\exists\, \mathbf{U}_{\mathcal{H}_Z} > 0$ *such that*

$$|\mathbb{M}(t) - \mathcal{K}(t)| \leq \mathcal{H}_Z(t) \mathbf{U}_{\mathcal{H}_Z} \varepsilon.$$

Definition 3.7. *The considered RRMS model will be a generalized UHRS if* $\exists\, \mathbf{U}_{\mathcal{H}_Z} > 0$ *such that*

$$|\mathbb{M}(t) - \mathcal{K}(t)| \leq \mathcal{H}_Z(t) \mathbf{U}_{\mathcal{H}_Z},$$

where $t \in [0, \boldsymbol{T}]$.

Remark 3.8. $\mathbb{M} \in A$ *be a solution of (3.11) if and only if* $\exists \mathscr{Q} \in A$, *the following properties hold:*

- $|\mathscr{Q}(t)| \leq \varepsilon$, $\mathscr{Q} = \max(\mathscr{Q}_i)^{\boldsymbol{T}}$ for $i = 1, 2, 3$.
- ${}^{c}D_{t}^{\mu}\mathbb{M}(t) = Z(t, \mathbb{M}(t)) + \mathscr{Q}(t)$.

Remark 3.9. $\mathbb{M} \in A$ *be a solution of (3.12) if and only if there exist* $\mathbb{H} \in A$, *the following properties hold:*

- $|\mathbb{H}(t)| \leq \varepsilon \mathcal{H}_Z(t), \mathbb{H} = \max(\mathbb{H}_i)^{\boldsymbol{T}}$, for $i = 1, 2, 3$.
- ${}^{c}D_{t}^{\mu}\mathbb{M}(t) = Z(t, \mathbb{M}(t)) + \mathbb{H}(t)$.

To concentrate our discussion on the Ulam's stabilities of the proposed model, we will first establish some necessary results. Additionally, we introduce an assumption that could prove useful in our subsequent analysis. We will assume that:

(A_3) $\forall\, t \in [0, \boldsymbol{T}]$, if $\exists$ an increasing function $\mathcal{H}_Z \in A$ and $\Pi_{\mathcal{H}_Z} > 0$ such that

$$\mathcal{I}_0^{\mu}\mathcal{H}_Z(t) \leq \Pi_{\mathcal{H}_Z}\mathcal{H}_Z(t).$$

Lemma 3.10. *For* $\mathbb{M} \in A$, *given inequality below holds:*

$$\left|\mathbb{M}(t) - \mathbb{M}_0 - \frac{1}{\Gamma(\mu)}\int_0^t (t-a)^{\mu-1} Z(a, \mathbb{M}(a))da\right| \leq \frac{\varepsilon t^{\mu}}{\Gamma(\mu+1)}.$$

Proof. Since $\mathbb{M} \in A$ satisfies (3.11), according to the 2nd condition of Remark 3.8, one can conclude that

$$\begin{cases} {}^{c}D_{t}^{\mu}\mathbb{M}(t) & = Z(t, \mathbb{M}(t)) + \mathscr{Q}(t), \\ \mathbb{M}(0) & = \mathbb{M}_0. \end{cases} \tag{3.14}$$

By utilizing the fractional integral, we can obtain the solution of system (3.14), which is expressed as follows:

$$\mathbb{M}(t) \;=\; \mathrm{m}_0 + \frac{1}{\Gamma(\mu)}\int_0^t (t-a)^{\mu-1} Z(a, \mathbb{M}(a))da + \frac{1}{\Gamma(\mu)}\int_0^t (t-a)^{\mu-1}\mathscr{Q}(a)da.$$

Based on the initial assumption, we can use the first condition of Remark 3.8 to obtain the following result:

$$\begin{aligned} \left|\mathbb{M}(t) - \mathbb{M}_0 - \frac{1}{\Gamma(\mu)}\int_0^t (t-a)^{\mu-1} Z(a, \mathbb{M}(a))da\right| &= \left|\frac{1}{\Gamma(\mu)}\int_0^t (t-a)^{\mu-1}\mathscr{Q}(a)da\right| \\ &\leq \frac{1}{\Gamma(\mu)}\int_0^t (t-a)^{\mu-1}|\mathscr{Q}(a)|\,da \\ &\leq \frac{\varepsilon t^{\mu}}{\Gamma(\mu+1)}. \end{aligned}$$

Hence, this ends the proof. □

Lemma 3.11. *If* $\mathbb{M} \in A$ *satisfies (3.12), then*

$$\left|\mathbb{M}(t) - \mathbb{M}_0 - \frac{1}{\Gamma(\mu)}\int_0^t (t-a)^{\mu-1} Z(a, \mathbb{M}(a))da\right| \leq \varepsilon\Pi_{\mathcal{H}_Z}\mathcal{H}_Z(t).$$

Proof. Let $\mathbb{M} \in A$ be the solution of (3.12). Using the second condition of Remark 3.9, we can express it as follows:

$$\mathbb{M}(t) = \mathbb{M}_0 + \frac{1}{\Gamma(\mu)} \int_0^t (t-a)^{\mu-1} Z(a, \mathbb{M}(a))da + \frac{1}{\Gamma(\mu)} \int_0^t (t-a)^{\mu-1} \mathbb{H}(a)da.$$

In the context of first part of Remark 3.9, we can express the above equation as:

$$\begin{aligned} \left|\mathbb{M}(t) - \mathbb{M}_0 - \mathcal{I}_0^{\eta} Z(t, \mathbb{M}(t))\right| &= \left|\mathcal{I}_0^{\mu} \mathbb{H}(t)\right| \\ &\leq \mathcal{I}_0^{\mu} \left|\mathbb{H}(t)\right| \\ &\leq \varepsilon^c \mathcal{I}_0^{\mu} \mathcal{H}_Z(t) \\ &\leq \varepsilon \Pi \mathcal{H}_Z(t). \end{aligned}$$

This ends the proof. □

Now, we are ready to verify the UH and Ulam-Hyers-Rassias (UHR) stability of the proposed RRMS model (3.1).

Theorem 3.12 (Generalized UHS)**.** *If the assertion* (A_1) *and* $\frac{\zeta_Z T^{\mu}}{\Gamma(\mu+1)} < 1$ *are fulfilled, then the proposed RRMS system (3.5) is a UHS and so, a generalized UHS.*

Proof. Let $\mathbb{M} \in A$ be any solution of Eq (3.11) and $\mathcal{K} \in A$ represent a unique solution of the proposed model (3.5), via Eq (3.6) and Lemma 3.10, one has

$$\begin{aligned} |\mathbb{M}(t) - \mathcal{K}(t)| &\leq \left|\mathbb{M}(t) - \mathcal{K}_0 - \frac{1}{\Gamma(\mu)} \int_0^t (t-a)^{\mu-1} Z(a, \mathcal{K}(a))da\right| \\ &\leq \left|\mathbb{M}(t) - \mathbb{M}_0 - \frac{1}{\Gamma(\mu)} \int_0^t (t-a)^{\mu-1} Z(a, \mathcal{K}(a))da\right| \\ &\quad + \frac{1}{\Gamma(\mu)} \int_0^t (t-a)^{\mu-1} \left|Z(\kappa, \mathbb{M}(a)) - Z(a, \mathcal{K}(a))\right| da \\ &\leq \left|\mathbb{M}(t) - \mathbb{M}_0 - \frac{1}{\Gamma(\mu)} \int_0^t (t-a)^{\mu-1} Z(a, \mathcal{K}(a))da\right| \\ &\quad + \frac{\zeta_Z}{\Gamma(\mu)} \int_0^t (t-a)^{\mu-1} \left|\mathbb{M}(a) - \mathcal{K}(a)\right| da \\ &\leq \frac{\varepsilon t^{\mu}}{\Gamma(\mu+1)} + \frac{\zeta_Z t^{\mu}}{\Gamma(\mu+1)} \left|\mathbb{M}(t) - \mathcal{K}(t)\right|. \end{aligned}$$

After simplification, we obtain $|\mathbb{M}(t) - \mathcal{K}(t)| \leq \varepsilon \mathcal{J}_Z$, where

$$\mathcal{J}_Z = \frac{\frac{t^{\mu}}{\Gamma(\mu+1)}}{1 - \frac{\zeta_Z t^{\mu}}{\Gamma(\mu+1)}}.$$

Therefore, the result of the UHS is achieved. Hence, the RRMS system (3.5) is a UHRS. Next, set $\mathcal{H}_Z(\varepsilon) = \varepsilon \mathcal{J}_Z$ so that $\mathcal{H}_Z(0) = 0$. Hence, the considered FO RRMS system is a generalized UHS. □

The given system exhibits a UHRS and a generalized UHRS according to the following theorem.

Theorem 3.13. *If (A_1), (A_3) and $\frac{\zeta_Z t^\mu}{\Gamma(\mu+1)} < 1$ are hold, then the model (3.5) is a UHRS, and accordingly, a generalized UHRS.*

Proof. Let $M \in A$ be any solution of (3.13), and $\mathcal{K} \in A$ denotes a unique solution of (3.5) via Eq (3.6) along with Lemma 3.11, one achieves

$$\begin{aligned}
|\mathbb{M}(t) - \mathcal{K}(t)| &\leq \left| \mathbb{M}(t) - \mathcal{K}_0 - \frac{1}{\Gamma(\mu)} \int_0^t (t-a)^{\mu-1} Z(a, \mathcal{K}(a)) da \right| \\
&\leq \left| \mathbb{M}(t) - \mathbb{M}_0 - \frac{1}{\Gamma(\mu)} \int_0^t (t-a)^{\mu-1} Z(a, \mathbb{M}(a)) da \right| \\
&\quad + \frac{1}{\Gamma(\mu)} \int_0^t (t-a)^{\mu-1} |Z(a, \mathbb{M}(a)) - Z(a, \mathcal{K}(a))| \, da \\
&\leq \left| \mathbb{M}(t) - \mathbb{M}_0 - \frac{1}{\Gamma(\mu)} \int_0^t (t-a)^{\mu-1} Z(a, \mathbb{M}(a)) da \right| \\
&\quad + \frac{\zeta_Z}{\Gamma(\mu)} \int_0^t (t-a)^{\mu-1} |\mathbb{M}(a) - \mathcal{K}(a)| \, da \\
&\leq \varepsilon \Pi_{\mathcal{H}_Z} \mathcal{H}_Z(t) + \frac{\zeta_Z t^\mu}{\Gamma(\mu+1)} |\mathbb{M}(t) - \mathcal{K}(t)| .
\end{aligned}$$

After simplification, one achieves $|\mathbb{M}(t) - \mathcal{K}(t)| \leq \frac{\varepsilon \Pi \mathcal{H}_Z(t)}{1 - \frac{\zeta_Z t^\mu}{\Gamma(\mu+1)}}$. By supposing:

$$\mathbf{U}_{\mathcal{H}_Z} = \frac{\Pi_{\mathcal{H}_Z}}{1 - \frac{\zeta_Z t^\mu}{\Gamma(\mu+1)}},$$

we get the required result:

$$|\mathbb{M}(t) - \mathcal{K}(t)| \leq \mathcal{H}_Z(t) \mathbf{U}_{\mathcal{H}_Z} \mu. \tag{3.15}$$

Consequently, the proposed system is a UHRS. Next, by setting $\varepsilon = 1$ in Eq (3.15) along with $\mathcal{H}_Z(0) = 0$, the suggested RRMS system is a generalized UHRS. □

3.4. Numerical results of RRMS model via Euler method

Finding exact or explicit solutions for FO differential equations remains a challenging task in computational and applied mathematics. In this section, we propose an approach to obtain approximate solutions for the FO model using fractional Euler's methods. These techniques focus on either the primary Taylor's function or a power series expansion. The strategy for the fractional Euler's numerical solution will be discussed.

By taking an IVP as

$$^C\mathcal{D}_t^\mu \mathbb{S}(t) = g\left(t, \mathbb{S}\left(t\right)\right), c \leq t \leq p, \mathbb{S}(t) = a, \tag{3.16}$$

where $c = t_0, t_1, ..., t_n = p$ such that $t_i = c + i \bigtriangledown$.

Let $j = 0, 1, 2, ..., n$, and $\bigtriangledown = \frac{p-c}{n}$.

Suppose that $^C\mathcal{D}_t^\mu \mathbb{S}(t)$ and $^C\mathcal{D}_t^{2\mu} \mathbb{S}(t)$ are continuous functions on $[c, p]$. Utilizing Taylor's expansion for $i = 0, 1, 2, ..., n$, one reaches:

$$\mathbb{S}\left(t_{i+1}\right) = \mathbb{S}\left(t_i + \bigtriangledown\right) = \mathbb{S}\left(t_i\right) + \frac{\bigtriangledown^\mu}{\mu} \left({}^C\mathcal{D}_t^\mu \mathbb{S}(t_i) \right) + \frac{\bigtriangledown^{2\mu}}{2\mu^2} \left({}^C\mathcal{D}_t^{2\mu} \mathbb{S} \right) (\zeta_i) ,$$

where $t_i < \zeta_i < t_{i+1}$. Since $\nabla = t_{i+1} - t_i$, there exist $\Phi_i \in (0, 1)$ such that

$$\mathbb{S}(t_{i+1}) = \mathbb{S}(t_i) + \frac{\nabla^{\mu}}{\mu}\left({}^{C}\mathcal{D}_t^{\mu}\mathbb{S}(t_i)\right) + \frac{\nabla^{2\mu}}{2\mu^2}\left({}^{C}\mathcal{D}_t^{2\mu}\mathbb{S}\right)(t_i + \Phi_i\nabla),$$

from which we have

$$\frac{\mu\left(\mathbb{S}(t_{i+1}) - \mathbb{S}(t_i)\right)}{\nabla^{\mu}} = g(t_i, \mathbb{S}(t_i)) + \frac{\nabla^{2\mu}}{2\mu^2}\left({}^{C}\mathcal{D}_t^{2\mu}\mathbb{S}\right)(t_i + \Phi_i\nabla). \tag{3.17}$$

For a small enough time interval, ∇, the term $\frac{\nabla^{2\mu}}{2\mu^2}\left({}^{C}\mathcal{D}_t^{2\mu}\mathbb{S}\right)(t_i + \Phi_i\nabla)$ in Eq (3.17) can be omitted. Therefore, from the Eq (3.17), we acquire the numerical method in the form of:

$$\mathbb{S}(t_{i+1}) = \mathbb{S}(t_i) + \frac{\nabla^{\mu}}{\mu}g(t_i, \mathbb{S}(t_i)). \tag{3.18}$$

Agarwal et al. utilized Euler's methods to develop a similar numerical scheme that provides the solution for Eq (3.16) in the following form:

$$\mathbb{S}(t_{i+1}) = \mathbb{S}(t_i) + \frac{\nabla^{\mu}}{\Gamma(\mu+1)}g(t_i, \mathbb{S}(t_i)). \tag{3.19}$$

The discrete Eqs (3.18) and (3.19) differ only in the denominator of their right-hand sides. In this paper, we utilize the numerical method presented in Eq (3.19) and can now employ the previous scheme for a simplified computation. We employ the numerical approximation scheme Eq (3.19), and each of the equations in the model (3.1). First, we consider the equation

$${}^{C}\mathcal{D}_t^{\mu}\mathbb{P}(t) = \gamma\mathbb{P}(1 - \mathbb{P}) - \beta\mathbb{P}\mathbb{Q},$$

for $0 < \mu < 1, t > 0$, with the initial values $\mathbb{S}(0) = \mathbb{S}_0 = 0.4$, $\mathbb{I}(0) = \mathbb{I}_0 = 0.3$, $\mathbb{Q}(0) = \mathbb{Q}_0 = 0.1$, the total population $\mathbb{N} = 0.8$.

Suppose $g(t, \mathbb{S}(t)) = \gamma\mathbb{P}(1 - \mathbb{P}) - \beta\mathbb{P}\mathbb{Q}$, then we define ${}^{C}\mathcal{D}_t^{\mu}\mathbb{P}(t) = g(t, \mathbb{S}(t))$ with $\mathbb{S}_0 = 0.4, 0 < \mu < 1, t > 0$. Next, utilizing the numerical scheme in Eq (3.19), one obtains

$$\mathbb{S}(t_{i+1}) = \mathbb{S}(t_i) + \frac{\nabla^{\mu}}{\Gamma(\mu+1)}g(t_i, \mathbb{S}(t_i)),$$

where $g(t_i, \mathbb{S}(t_i))$ is described as

$$g(t_i, \mathbb{S}(t_i)) = \gamma\mathbb{P}(t_i)(1 - \mathbb{P}(t_i)) - \beta\mathbb{P}(t_i)\mathbb{Q}(t_i),$$

for $i = 0, 1, 2, 3, ..., n - 1$.

Now,

$${}^{C}\mathcal{D}_t^{\mu}\mathbb{I}(t_i) = \beta\mathbb{P}(t_i)\mathbb{Q}(t_i) - \alpha\mathbb{I}(t_i).$$

Let $g(t, \mathbb{I}(t_i)) = \beta\mathbb{P}(t_i)\mathbb{Q}(t_i) - \alpha\mathbb{I}(t_i)$, and define ${}^{C}\mathcal{D}_t^{\mu}\mathbb{I}(t_i) = g(t, \mathbb{I}(t_i))$ where $\mathbb{I}_0 = 0.3, 0 < \mu < 1, t > 0$. Utilizing the numerical solution scheme in Eq (3.10), we obtain

$$\mathbb{I}(t_{i+1}) = \mathbb{I}(t_i) + \frac{\nabla^{\mu}}{\Gamma(\mu+1)}g(t_i, \mathbb{I}(t_i)),$$

where $g(t_i, \mathbb{I}(t_i))$ is described as

$$g(t_i, \mathbb{I}(t_i)) = \beta\mathbb{P}(t_i)\mathbb{Q}(t_i) - \alpha\mathbb{I}(t_i),$$

for $i = 0, 1, 2, ..., n-1$. Lastly,

$${}^{C}\mathcal{D}_t^{\mu}\mathbb{Q}(t) = \delta\mathbb{I}(t) - d\mathbb{P}(t)\mathbb{Q}(t) - \kappa\mathbb{Q}(t).$$

Suppose $g(t_i, \mathbb{Q}(t_i)) = \delta\mathbb{I}(t_i) - d\mathbb{P}(t_i)\mathbb{Q}(t_i) - \kappa\mathbb{Q}(t_i)$, define as ${}^{C}\mathcal{D}_t^{\mu}\mathbb{Q}(t) = g(t_i, \mathbb{I}(t_i))$, where $\mathbb{Q}_0 = 0.1, 0 < \mu < 1, t > 0$.

Utilizing the numerical scheme in Eq (3.10), we obtain

$$\mathbb{Q}(t_{i+1}) = \mathbb{Q}(t_i) + \frac{\nabla^{\mu}}{\Gamma(\mu+1)} g(t_i, \mathbb{Q}(t_i)),$$

where $g(t_i, \mathbb{Q}(t_i))$ is described as

$$g(t_i, \mathbb{Q}(t_i)) = \delta\mathbb{I}(t_i) - d\mathbb{P}(t_i)\mathbb{Q}(t_i) - \kappa\mathbb{Q}(t_i),$$

for $i = 0, 1, 2, ..., n-1$.

4. Numerical simulations

This section presents a simulation of the proposed mathematical model to analyze the behavior of three classes of a system for different cases. The initial conditions for these cases are chosen as $\mathbb{P} = 0.4, \mathbb{I} = 0.3$, and $\mathbb{Q} = 0.1$. The three cases correspond to the disease-free equilibrium (DFE) point, the endemic equilibrium (EE) point, and oscillatory dynamics of the disease. For the DFE point simulation, we use specific parameter values such as $\gamma = 1.5, \beta = 0.25, \alpha = 1.13, \delta = 0.2, d = 0.01$, and $\kappa = 0.1$. The simulation results are presented in Figure 1, where sub-figures (a)–(c) display the geometry of normal brain cells (NBC), infected brain cells (IBC), and damaged brain cells (DBC) for a few FOs.

For the EE point simulation, we use a different set of parameter values such as $\gamma = 0.5, \beta = 0.28, \alpha = 0.13, \delta = 0.1, d = 0.01$, and $\kappa = 0.1$. The results of this simulation are presented in Figure 2, where sub-figures (a)–(c) show the disease dynamics for some FOs. For the oscillatory dynamics simulation, we use a set of parameter values such as $\gamma = 0.5, \beta = 1.25, \alpha = 0.13, \delta = 0.1, d = 0.01$, and $\kappa = 0.1$. The simulation results reveal that the system exhibits oscillatory dynamics of the considered disease, and this behavior is presented in Figure 3, where sub-figures (a)–(c) depict the evolution of each class of the proposed model for a few FOs.

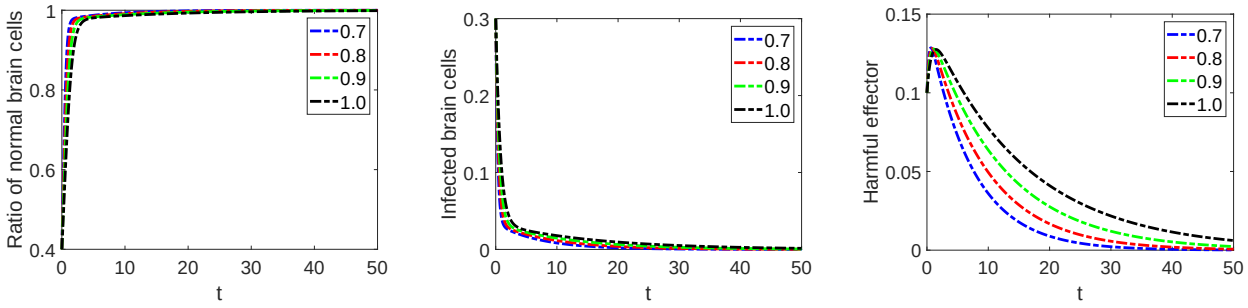

Figure 1. Graphs of the proposed system for DFE at $\gamma = 1.5, \beta = 0.25, \alpha = 1.13, \delta = 0.2, d = 0.01$, and $\kappa = 0.1$.

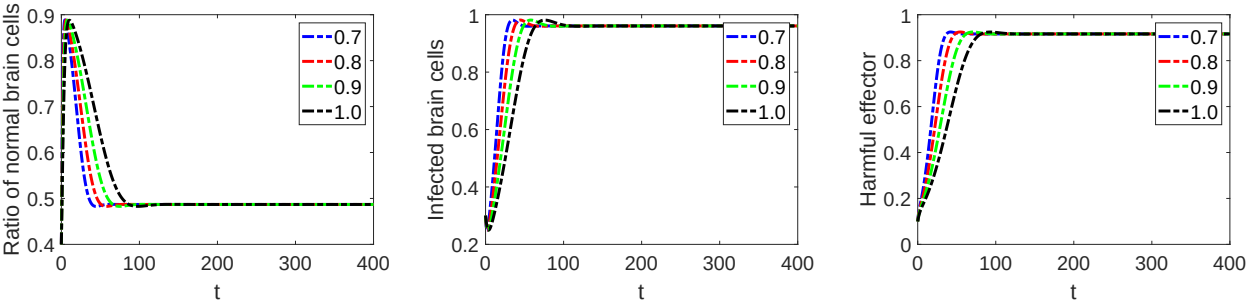

Figure 2. Graphs of the proposed system for EE at $\gamma = 0.5, \beta = 0.28, \alpha = 0.13, \delta = 0.1, d = 0.01$, and $\kappa = 0.1$.

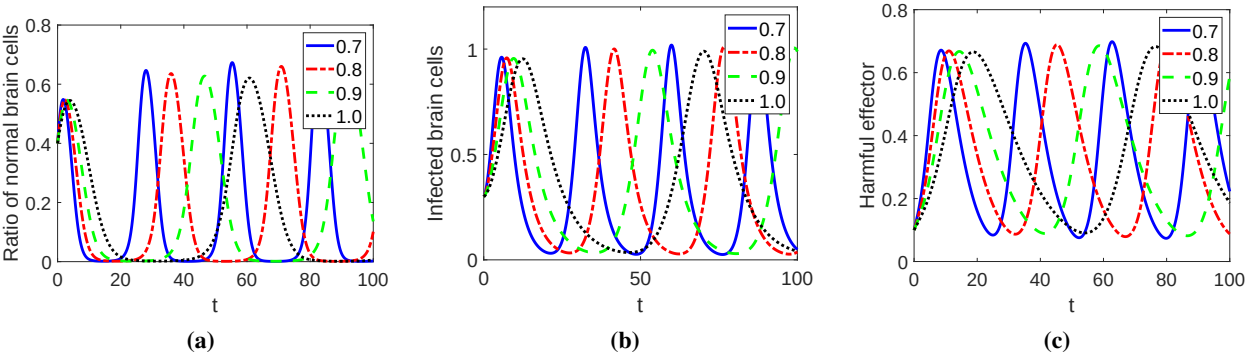

Figure 3. Oscillatory dynamics of the proposed system for $\gamma = 0.5, \beta = 1.25, \alpha = 0.13, \delta = 0.1, d = 0.01$, and $\kappa = 0.1$.

This section presents a simulation of the proposed mathematical model to analyze the behavior of three classes of a system for different cases. The initial conditions for these cases are chosen as $\mathbb{P} = 0.4, \mathbb{I} = 0.3$, and $\mathbb{Q} = 0.1$. The three cases correspond to the disease-free equilibrium (DFE)

point, the endemic equilibrium (EE) point, and oscillatory dynamics of the disease. For the DFE point simulation, we use specific parameter values such as $\gamma = 1.5, \beta = 0.25, \alpha = 1.13, \delta = 0.2, d = 0.01$, and $\kappa = 0.1$. The simulation results are presented in Figure 1, where sub-figures $(a) - (c)$ display the geometry of normal brain cells (NBC), infected brain cells (IBC), and damaged brain cells (DBC) for a few FOs.

For the EE point simulation, we use a different set of parameter values such as $\gamma = 0.5, \beta = 0.28, \alpha = 0.13, \delta = 0.1, d = 0.01$, and $\kappa = 0.1$. The results of this simulation are presented in Figure 2, where sub-figures $(a) - (c)$ show the disease dynamics for some FOs. For the oscillatory dynamics simulation, we use a set of parameter values such as $\gamma = 0.5, \beta = 1.25, \alpha = 0.13, \delta = 0.1, d = 0.01$, and $\kappa = 0.1$. The simulation results reveal that the system exhibits oscillatory dynamics of the considered disease, and this behavior is presented in Figure 3, where sub-figures $(a) - (c)$ depict the evolution of each class of the proposed model for a few FOs.

Furthermore, we analyze the chaotic dynamics of the proposed model in Figures 4 and 5. We choose different values of FO to illustrate the memory and heredity features of the model. From these simulations, we observe that the evolution of the disease varies as the value of the FO changes. We note that the model achieves stability more rapidly at lower FOs compared to higher orders. Moreover, the graphs of each class get closer to the dynamics of the integer order model as the FO increases. Therefore, we conclude that the proposed model is more advanced and generalized than the classical model.

From a biological perspective, mathematical models are an important tool to study the dynamics of diseases and can help to understand how they spread and how they can be controlled. The proposed model is used to simulate the behavior of a disease affecting brain cells. The simulations provide insight into how the disease progresses under different conditions, such as at the DFE point, the EE point, and with oscillatory dynamics. We also analyze the chaotic dynamics of the model and how the disease evolution changes as the value of the FO changes. These findings could provide valuable information for developing strategies to control and treat the disease.

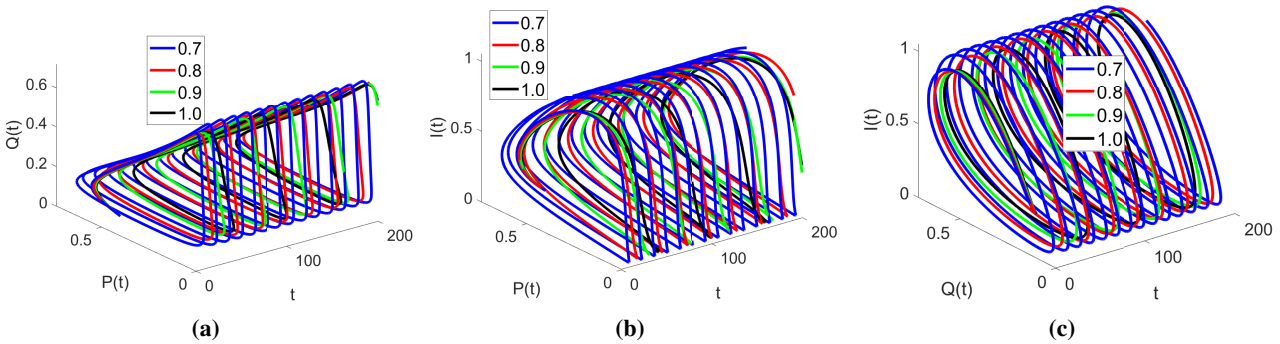

Figure 4. Complex dynamics of the proposed system for $\gamma = 0.5, \beta = 1.25, \alpha = 0.13, \delta = 0.1, d = 0.01$, and $\kappa = 0.1$.

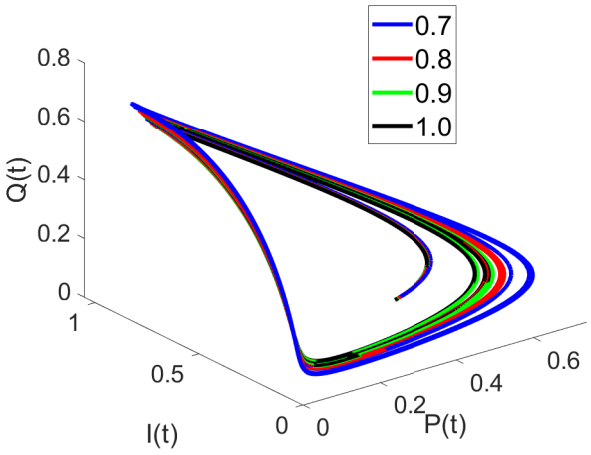

Figure 5. Chaotic dynamics of the proposed system for $\gamma = 0.5, \beta = 1.25, \alpha = 0.13, \delta = 0.1, d = 0.01$, and $\kappa = 0.1$.

5. Conclusions and future recommendation

In this research, we have explored a mathematical model to assess the level of disease progression and recurrence. To provide non-negative solutions, we have expanded the model by including Caputo fractional-order derivative operators. Additionally, we have also established steady-state points and basic reproductive number. Moreover, we have identified the necessary conditions for the existence of a unique fractional system. Different forms of UHS have been demonstrated to show that the solution of the considered FO system is a UHS. To obtain an approximate solution for the FO system, we have used an effective Euler-type numerical technique.

The study presents the results of three different cases, where the behavior of the model is analyzed for a few fractional values. We have concluded that the proposed system is more generalized than the classical model, as it provides the behavior of the model for fractional values. Overall, this research contributes to the understanding of disease progression and recurrence by providing a mathematical model that can be utilized to simulate and analyze the behavior of disease models. The inclusion of Caputo fractional-order derivative operators allows for a more comprehensive analysis of the model's stability and recurrence, making it a valuable tool for researchers and health care professionals.

In the near future, we will study the proposed model using different operators and concepts, such as fractal fractional operators, fuzzy operators, and stochastic concepts.

Use of AI tools declaration

The authors declare they have not used Artificial Intelligence (AI) tools in the creation of this article.

Acknowledgments

Princess Nourah bint Abdulrahman University Researchers Supporting Project number (PNURSP2023R8). Princess Nourah bint Abdulrahman University, Riyadh, Saudi Arabia.

Conflict of interest

There exist no conflict of interest regarding to this research work.

References

1. N. Shigesi, M. Kvaskoff, S. Kirtley, Q. Feng, H. Fang, J. C. Knight, et al., The association between endometriosis and autoimmune diseases: a systematic review and meta-analysis, *Hum. Reprod. Update*, **25** (2019), 486–503. http://doi.org/10.1093/humupd/dmz014
2. R. Nardone, V. Versace, L. Sebastianelli, F. Brigo, S. Golaszewski, M. Christova, et al., Transcranial magnetic stimulation and bladder function: a systematic review, *Clin. Neurophysiol.*, **130** (2019), 2032–2037. http://doi.org/10.1016/j.clinph.2019.08.020
3. I. J. Crane, J. V. Forrester, Th1 and Th2 lymphocytes in autoimmune disease, *Crit. Rev. Immunol.*, **25** (2005), 75–102. http://doi.org/10.1615/critrevimmunol.v25.i2.10
4. Z. Blach-Olszewska, J. Leszek, Mechanisms of over-activated innate immune system regulation in autoimmune and neurodegenerative disorders, *Neuropsych. Dis. Treat.*, **3** (2007), 365–372. http://doi.org/10.2147/ndt.s12160184
5. G. E. Kaiko, J. C. Horvat, K. W. Beagley, P. M. Hansbro, Immunological decision-making: how does the immune system decide to mount a helper T-cell response, *Immunology*, **123** (2007), 326–338. http://doi.org/10.1111/j.1365-2567.2007.02719.x
6. P. Blanco, A. K. Palucka, V. Pascual, J. Banchereau, Dendritic cells and cytokines in human inflammatory and autoimmune diseases, *Cytokine Growth Factor Rev.*, **19** (2008), 41–52. http://doi.org/10.1016/j.cytogfr.2007.10.004
7. J. Tabarkiewicz, K. Pogoda, A. Karczmarczyk, P. Pozarowski, K. Giannopoulos, The role of IL-17 and Th17 lymphocytes in autoimmune diseases, *Arch. Immunol. Ther. Exp.*, **63** (2015), 435–449. http://doi.org/10.1007/s00005-015-0344-z
8. B. B. Ganesh, P. Bhattacharya, A. Gopisetty, B. S. Prabhakar, Role of cytokines in the pathogenesis and suppression of thyroid autoimmunity, *J. Interferon Cytokine Res.*, **31** (2011), 721–731. http://doi.org/10.1089/jir.2011.0049
9. F. D. Lublin, S. C. Reingold, J. A. Cohen, G. R. Cutter, P. S. Sørensen, A. J. Thompson, et al., Defining the clinical course of multiple sclerosis: the 2013 revisions, *Neurology*, **83** (2014), 278–286. http://doi.org/10.1212/WNL.0000000000000560
10. R. Zivadinov, R. Bakshi, Central nervous system atrophy and clinical status in multiple sclerosis, *J. Neuroimaging*, **14** (2004), 27s–35s. http://doi.org/10.1177/1051228404266266
11. T. Akaishi, I. Nakashima, S. Mugikura, M. Aoki, K. Fujihara, Whole-brain and grey matter volume of Japanese patients with multiple sclerosis, *J. Neuroimmunol.*, **306** (2017), 68–75. http://doi.org/10.1016/j.jneuroim.2017.03.009
12. D. T. Chard, C. M. Griffin, G. J. M. Parker, R. Kapoor, A. J. Thompson, D. H. Miller, Brain atrophy in clinically early relapsing remitting-multiple sclerosis, *Brain*, **125** (2002), 327–337. http://doi.org/10.1093/brain/awf025

13. C. H. Polman, S. C. Reingold, B. Banwell, M. Clanet, J. A. Cohen, M. Filippi, et al., Diagnostic criteria for multiple sclerosis: 2010 revisions to the McDonald criteria, *Ann. Neurol.*, **69** (2011), 292–302. http://doi.org/10.1002/ana.22366

14. H. H. Uhlig, B. S. McKenzie, S. Hue, C. Thompson, B. J. Shaikh, R. Stepankova, et al., Differential activity of IL-12 and IL-23 in mucosal and systemic innate immune pathology, *Immunity*, **25** (2006), 309–318. http://doi.org/10.1016/j.immuni.2006.05.017

15. R. H. Khonsari, V. Calvez, The origins of concentric demyelination: self-organization in the human brain, *PLoS ONE*, **2** (2007), e150. https://doi.org/10.1371/journal.pone.0000150

16. M. C. Lombardo, R. Barresi, E. Bilotta, F. Gargano, P. Pantano, M. Sammartino, Demyelination patterns in a mathematical model of multiple sclerosis, *J. Math. Biol.*, **75** (2017), 373–417. https://doi.org/10.1007/s00285-016-1087-0

17. M. F. Elettreby, E. Ahmed, A simple mathematical model for relapsing remitting multiple sclerosis (RRMS), *Med. Hypotheses*, **135** (2020), 109478. https://doi.org/10.1016/j.mehy.2019.109478

18. K. Shah, M. A. Alqudah, F. Jarad, T. Abdeljawad, Semi-analytical study of Pine Wilt Disease model with convex rate under Caputo-Febrizio fractional-order derivative, *Chaos Soliton. Fract.*, **135** (2020), 109754. https://doi.org/10.1016/j.chaos.2020.109754

19. K. Shah, T. Abdeljawad, Study of a mathematical model of COVID-19 outbreak using some advanced analysis, *Wave. Random Complex*, **2022** (2022), 1–18. https://doi.org/10.1080/17455030.2022.2149890

20. C. Xu, D. Mu, Z. Liu, Y. Pang, M. Liao, C. Aouiti, New insight into bifurcation of fractional-order 4D neural networks incorporating two different time delays, *Commun Nonlinear Sci.*, **118** (2023) 107043. https://doi.org/10.1016/j.cnsns.2022.107043

21. C. Xu, Z. Liu, P. Li, J. Yan, L. Yao, Bifurcation mechanism for fractional-order three-triangle multi-delayed neural networks, *Neural Process. Lett.*, **2022** (2022), 1–27. https://doi.org/10.1007/s11063-022-11130-y

22. C. Xu, W. Zhang, C. Aouiti, Z. Liu, L. Yao, Bifurcation insight for a fractional-order stage-structured predator-prey system incorporating mixed time delays, *Math. Method. Appl. Sci.*, **46** (2023), 9103–9118. https://doi.org/10.1002/mma.9041

23. C. Xu, M. Liao, P. Li, Y. Guo, Z. Liu, Bifurcation properties for fractional order delayed BAM neural networks, *Cogn. Comput.*, **13** (2021), 322–356. https://doi.org/10.1007/s12559-020-09782-w

24. A. Khan, A. Ali, S. Ahmad, S. Saifullah, K. Nonlaopon, A. Akgul, Nonlinear Schrödinger equation under non-singular fractional operators: a computational study, *Results Phys.*, **43** (2022) 106062. https://doi.org/10.1016/j.rinp.2022.106062

25. K. S. Nisar, A. Ciancio, K. K. Ali, M. S. Osman, C. Cattani, D. Baleanu, et al., On beta-time fractional biological population model with abundant solitary wave structures, *Alex. Eng. J.*, **61** (2022), 1996–2008. https://doi.org/10.1016/j.aej.2021.06.106

26. O. A. Arqub, M. Al-Smadi, H. Almusawa, D. Baleanu, T. Hayat, M. Alhodaly, et al., A novel analytical algorithm for generalized fifth-order time-fractional nonlinear evolution equations with conformable time derivative arising in shallow water waves, *Alex. Eng. J.*, **61** (2022), 5753–5769. https://doi.org/10.1016/j.aej.2021.12.044

27. B. C. Barro, M. A. Taneco-Hernández, Y. P. Lv, J. F. Gómez-Aguilar, M. S. Osman, H. Jahanshahi, et al., Analytical solutions of fractional wave equation with emory effect using the fractional derivative with exponential kernel, *Results Phys.*, **25** (2021), 104148. https://doi.org/10.1016/j.rinp.2021.104148

28. S. Rashid, K. T. Kubra, S. Sultana, P. Agarwal, M. S. Osman, An approximate analytical view of physical and biological models in the setting of Caputo operator via Elzaki transform decomposition method, *J. Comput. Appl. Math.*, **413** (2022), 114378. https://doi.org/10.1016/j.cam.2022.114378

29. T. Ak, M. S. Osman, A. H. Kara, Polynomial and rational wave solutions of Kudryashov-Sinelshchikov equation and numerical simulations for its dynamic motions, *J. Appl. Anal. Comput.*, **10** (2020), 2145–2162. https://doi.org/10.11948/20190341

30. K. Iskakova, M. M. Alam, S. Ahmad, S. Saifullah, A. Akgul, G. Yilmaz, Dynamical study of a novel 4D hyperchaotic system: an integer and fractional order analysis, *Math. Comput. Simulat.*, **208** (2023), 219–245. https://doi.org/10.1016/j.matcom.2023.01.024

31. S. A. M. Abdelmohsen, S. Ahmad, M. F. Yassen, S. A. Asiri, A. M. M. Ashraf, S. Saifullah, et al., Numerical analysis for hidden chaotic behavior of a coupled memristive dynamical system via fractal-fractional operator based on newton polynomial interpolation, *Fractals*, **2023** (2023), 1–24. https://doi.org/10.1142/S0218348X2340087X

32. X. W. Jiang, J. H. Li, B. Li, W. Yin, L. Sun, X. Y. Chen, Bifurcation, chaos, and circuit realisation of a new four-dimensional memristor system, *Int. J. Nonlin. Sci. Num.*, **2022** (2022), 0393. https://doi.org/10.1515/ijnsns-2021-0393

33. B. Li, Z. Eskandari, Z. Avazzadeh, Strong resonance bifurcations for a discrete-time prey-predator model, *J. Appl. Math. Comput.*, **2023** (2023), 2. https://doi.org/10.1007/s12190-023-01842-2

34. B. Li, Z. Eskandari, Z. Avazzadeh, Dynamical behaviors of an SIR epidemic model with discrete time, *Fractal Fract.*, **6** (2022), 659. https://doi.org/10.3390/fractalfract6110659

35. S. Saifullah, S. Ahmad, F. Jarad, Study on the dynamics of a piecewise Tumour-Immune interaction model, *Fractals*, **30** (2022), 2240233. https://doi.org/10.1142/S0218348X22402332

36. H. Qu, M. U. Rahman, S. Ahmad, M. B. Riaz, M. Ibrahim, T. Saeed, Investigation of fractional order bacteria dependent disease with the effects of different contact rates, *Chaos Soliton. Fract.*, **159** (2022), 112169. https://doi.org/10.1016/j.chaos.2022.112169

37. Z. H. Shen, Y. M. Chu, M. A. Khan, S. Muhammad, O. A. Al-Hartomy, M. Higazy, Mathematical modeling and optimal control of the COVID-19 dynamics, *Results Phys.*, **31** (2021), 105028. https://doi.org/10.1016/j.rinp.2021.105028

38. Y. M. Chu, M. Farhan, M. A. Khan, M. Y. Alshahrani, T. Muhammad, S. Islam, Mathematical modeling and stability analysis of Buruli ulcer in Possum mammals, *Results Phys.*, **27** (2021), 104471. https://doi.org/10.1016/j.rinp.2021.104471

39. Y. M. Chu, A. Ali, M. A. Khan, S. Islam, S. Ullah, Dynamics of fractional order COVID-19 model with a case study of Saudi Arabia, *Results Phys.*, **21** (2021), 103787. https://doi.org/10.1016/j.rinp.2020.103787

40. W. Y. Shen, Y. M. Chu, M. U. Rahman, I. Mahariq, A. Zeb, Mathematical analysis of HBV and HCV co-infection model under nonsingular fractional order derivative, *Results Phys.*, **28** (2021), 104582. https://doi.org/10.1016/j.rinp.2021.104582

41. Y. M. Chu, M. F. Khan, S. Ullah, S. A. A. Shah, M. Farooq, M. B. Mamat, Mathematical assessment of a fractional-order vector-host disease model with the Caputo-Fabrizio derivative, *Math. Method. Appl. Sci.*, **46** (2023), 232–247. https://doi.org/10.1002/mma.8507

42. L. V. C. Hoan, M. A. Akinlar, M. Inc, J. F. Gómez-Aguilar, Y. M. Chu, B. Almohsen, A new fractional-order compartmental disease model, *Alex. Eng. J.*, **59** (2020), 3187–3196. https://doi.org/10.1016/j.aej.2020.07.040

43. Y. M. Chu, M. S. Khan, M. Abbas, S. Ali, W. Nazeer, On characterizing of bifurcation and stability analysis for time fractional glycolysis model, *Chaos Soliton. Fract.*, **165** (2022), 112804. https://doi.org/10.1016/j.chaos.2022.112804

44. J. Fang, Z. S. Qian, Y. M. Chu, M. U. Rahman, On nonlinear evolution model for drinking behavior under Caputo-Fabrizio derivative, *J. Appl. Anal. Comput.*, **12** (2022), 790–806. https://doi.org/10.11948/20210357

45. D. Baleanu, K. Diethelm, E. Scalas, J. J. Trujillo, *Fractional calculus: models and numerical methods*, Singapore: World Scientific, 2012. https://doi.org/10.1142/10044

AIMS Press